Acta Cryst. (1989). B45, 457–462

A Re-examination of the Lisicon Structure Using High-Resolution Powder Neutron Diffraction: Evidence for Defect Clustering

BY I. ABRAHAMS AND P. G. BRUCE*

Department of Chemistry, Heriot-Watt University, Riccarton, Edinburgh EH14 4AS, Scotland

W. I. F. DAVID

Rutherford–Appleton Laboratory, SERC, Chilton, Didcot, Oxon OX11 0QX, England

AND A. R. WEST

Department of Chemistry, University of Aberdeen, Meston Walk, Old Aberdeen AB9 2UE, Scotland

(*Received* 4 *February* 1989; *accepted* 19 *May* 1989)

Abstract

The structure of $Li_3Zn_{0.5}GeO_4$, which is an interstitial solid solution $Li_{(2+2x)}Zn_{(1-x)}GeO_4$ ($x = 0.5$), has been re-examined using the high-resolution time-of-flight powder neutron diffractometer (HRPD) at ISIS, Rutherford–Appleton Laboratory. All measurements were obtained at room temperature. The structure has been refined, using a modified Rietveld method, in the orthorhombic space group *Pnma* (No. 62) with cell dimensions $a = 10.8523$ (1), $b = 6.27431$ (7) and $c = 5.15807$ (6) Å; $Z = 4$, $V = 353.42$ Å^3, $D_x = 3.57$ g cm^{-3}, $M_r = 190.1$. The final R factors were $R_{wp} = 6.73$, $R_{ex} = 6.84\%$. The structure is based on an oxide-ion array which is between hexagonal and tetragonal packing. Germanium and zinc ions are located in tetrahedral sites with lithium distributed over both tetrahedral and octahedral sites. Previous studies have identified only one octahedral interstitial site for Li^+ ions but there is evidence for the occupation of a second such site in this refinement. A model involving two types of defect cluster, which accommodate all of the interstitial octahedral lithium ions, is proposed. The HRPD data are compared with a previous structure refinement using constant-wavelength powder neutron diffraction on the D1A diffractometer at ILL, Grenoble. Considerable improvement is noted in the accuracy of the refined parameters.

Introduction

Accurate structure determination of crystalline solid electrolytes is essential if the general features of the ionic conduction process in such systems are to be understood. It is particularly important that the distribution of mobile ions within the semi-rigid crystalline framework is defined as precisely as possible. Diffraction methods are, in the case of crystalline solids, paramount among the armoury of techniques available for structure elucidation.

Lisicon is the generic name applied to a range of solid solutions based on the γ_{II}-polymorph of Li_2ZnGeO_4, which is itself isostructural with γ-Li_3PO_4. The interstitial solid solutions $Li_{(2+2x)}Zn_{(1-x)}GeO_4$ ($0 < x < 0.87$) are good lithium-ion conductors capable of exhibiting conductivities of $0.13\ \Omega^{-1}\ cm^{-1}$ at 573 K (Hong, 1978), whereas the vacancy solid solutions ($-0.36 < x < 0$) are not (Bruce & West, 1982). There are now many lithium-ion-conducting solids known which are essentially isostructural with lisicon (Rodger, Kuwano & West, 1985).

Single-crystal X-ray diffraction has been used to determine the structures of two compositions, $x = 0.5$ (Plattner & Völlenkle, 1979) and 0.75 (Hong, 1978), within the lisicon interstitial solid-solution system. However, the relatively weak X-ray scattering factors for lithium ions place the technique at a disadvantage when accurate lithium-ion distributions are required, as in the case of the lisicon solid solutions. For this reason we previously investigated the structure of the interstitial solid solutions using powder neutron diffraction, on the D1A diffractometer at ILL, Grenoble, which led to a more precise structural model (Abrahams, Bruce, David & West, 1988). The refined structure includes lithium ions distributed over several sites within the oxygen sublattice. Although this neutron refinement clarified certain structural features that were not evident in the previous X-ray studies, the availability of the new high-resolution powder neutron diffractometer (HRPD) at ISIS, Rutherford–Appleton Laboratory, with its high resolution and q range, encouraged us to re-evaluate the structure of these solid electrolytes. Here we present the improved structure refinement, using HRPD, of one member of the lisicon solid

* Author to whom correspondence should be addressed.

0108-7681/89/050457-06$03.00

solution series $Li_3Zn_{0.5}GeO_4$. The re-examination has identified a new interstitial site for mobile lithium ions not previously observed at this composition, and indicates the existence of defect clusters. In addition we offer a comparison between the structures refined using D1A and HRPD which indicates that the latter instrument is very well suited to refinement of highly disordered structures. We have chosen the $x = 0{\cdot}5$ composition, $Li_3Zn_{0.5}GeO_4$, because it exhibits the greatest thermodynamic stability of any of the solid-solution compositions as shown by the Li_4GeO_4–$ZnGeO_4$ phase diagram (Bruce & West, 1980).

Experimental

Preparation

$Li_3Zn_{0.5}GeO_4$ was prepared by solid-state reaction between Li_2CO_3, GeO_2 and ZnO. Starting materials were ground up as a slurry in ethanol for 15 min. The dried powder was pressed into a pellet, heated in a gold boat in air for 2 h at 923 K to decompose the carbonate, and then at 1103 K for 2 h before quenching to room temperature. After preliminary experiments these conditions were found to provide a product of high purity as determined by powder X-ray diffraction using a Stöe–Guinier camera.

Data collection

A high-resolution time-of-flight (t.o.f.) powder neutron diffraction profile was collected on the HRPD diffractometer at ISIS, Rutherford–Appleton Laboratory. This instrument possesses a theoretical resolution $\Delta d/d$ of 5×10^{-4}, and a range of d spacings from 0·4 to 6 Å may be examined. A sample position 1 m in front of the bank of back-scattering detectors was used for the experiment. Approximately 10 g of powdered $Li_3Zn_{0.5}GeO_4$ were placed in an aluminium sample can with vanadium windows and data collected in the t.o.f. range 20–120×10^3 μs. The data were fitted using a modified Rietveld method with the peak shape modelled by a convolution of Gaussian and two exponential functions (David, Akporiaye, Ibberson & Wilson, 1988). The scattering lengths used were Ge 0·8193, O 0·5805, Li −0·220, Zn 0·5680 $\times 10^{-12}$ cm (Koester & Rauch, 1981).

Structure refinement

The structure of $Li_3Zn_{0.5}GeO_4$ was refined in the orthorhombic space group *Pnma* (No. 62) (*International Tables for Crystallography,* 1983), using the previous structure refinement by powder neutron diffraction (Abrahams, Bruce, David & West, 1988) as a starting model. The scale and zero-point parameters were refined first, followed, in subsequent refinements, by the unit-cell dimensions, four background parameters and the half width of the Gaussian part of the peak shape. Germanium and oxygen positional parameters were then refined followed by those for lithium and zinc. Both lithium and zinc ions occupy two sets of tetrahedral sites labelled Li/Zn(1) and Li/Zn(2) in Table 1. The zinc occupancy was allowed to vary between the two sites with the overall occupancy fixed at the value determined by the composition of the solid solution. Initially, the lithium occupancy on site (1) was allowed to vary independently; however, it refined to a value such that the sum of the lithium and zinc occupancies on that site was close to unity. Therefore, in subsequent refinements the total occupancy of this site was fixed at one. A third tetrahedral site Li(2a), which shares a face with the Li/Zn(2) site, is also occupied by lithium ions; the distance between the centres of these sites is approximately 1 Å and, consequently, the sites cannot be simultaneously occupied. Therefore lithium occupancies of sites (2) and (2a) were refined assuming that the total amount of lithium and zinc distributed over the (2) and (2a) sites was fixed at unity.

Four octahedrally coordinated sites are possible in this structure; lithium occupancy was found in two of these sites designated Li(3) and Li(4). Initially, Li(3) was located on the 4(*c*) position (0·20, 0·25, 0·0) as indicated in the previous structure refinement; however, by allowing all of its positional parameters to refine, the Li(3) ion moved off the special position and onto an eightfold general position. In the final refinement the octahedral Li ions were allowed to adjust their occupanices between Li(3) and Li(4) sites; the total lithium content of the unit cell was fixed at that determined by the composition

Table 1. *Refined cell and atomic parameters for* $Li_3Zn_{0.5}GeO_4$ *with estimated standard deviations in parentheses*

$a = 10{\cdot}8523$ (1), $b = 6{\cdot}27431$ (7), $c = 5{\cdot}15807$ (6) Å.

	Position	x	y	z	B(Å^2)	Occupancy
Ge	4(*c*)	0·4133 (6)	0·25	0·3335 (2)	—	1
O(1)	8(*d*)	0·3360 (1)	0·0230 (2)	0·2171 (2)	-	1
O(2)	4(*c*)	0·0875 (2)	0·75	0·1714 (3)	-	1
O(3)	4(*c*)	0·0652 (1)	0·25	0·2797 (3)	-	1
Li(1)	4(*c*)	0·4298 (8)	0·75	0·183 (2)	2·8 (3)	0·905 (6)
Zn(1)	4(*c*)	0·4298 (8)	0·75	0·183 (2)	2·8 (3)	0·095 (6)
Li(2)	8(*d*)	0·141 (2)	−0·039 (4)	0·356 (6)	2·7 (4)	0·647 (9)
Zn(2)	8(*d*)	0·141 (2)	−0·039 (4)	0·356 (6)	2·7 (4)	0·202 (3)
Li(2a)	8(*d*)	0·167 (2)	0·030 (3)	0·212 (5)	2·7 (4)	0·156 (9)
Li(3)	8(*d*)	0·204 (1)	0·206 (3)	−0·009 (3)	3·5 (3)	0·210 (4)
Li(4)	4(*b*)	0·0	0·0	0·5	3·5 (3)	0·081 (9)

Anisotropic thermal parameters (Å^2)

	B_{11}	B_{22}	B_{33}	B_{23}	B_{13}	B_{12}
Ge	0·89 (4)	1·17 (5)	0·96 (5)	—	0·05 (5)	—
O(1)	0·88 (4)	1·79 (5)	1·54 (5)	−0·49 (4)	0·02 (4)	−0·21 (4)
O(2)	1·10 (6)	1·11 (6)	0·79 (6)	-	0·15 (6)	—
O(3)	0·60 (6)	1·36 (6)	1·42 (7)	—	−0·05 (5)	-

Table 2. *Bond lengths and significant contact distances* (Å) *for* $Li_3Zn_{0.5}GeO_4$ *with estimated standard deviations in parentheses*

Ge—O(1)	1·759 (1)	Li(1)/Zn(1)—O(1)	2·000 (4)
Ge—O(1′)	1·759 (1)	Li(1)/Zn(1)—O(1′)	2·000 (4)
Ge—O(2)	1·743 (2)	Li(1)/Zn(1)—O(2)	1·869 (8)
Ge—O(3)	1·749 (2)	Li(1)/Zn(1)—O(3)	2·079 (9)
Li/Zn(2)—O(1)	1·88 (3)	Li(2a)—O(1)	2·57 (3)
Li/Zn(2)—O(1′)	2·26 (3)	Li(2a)—O(1′)	1·83 (3)
Li/Zn(2)—O(2)	1·73 (3)	Li(2a)—O(2)	1·97 (2)
Li/Zn(2)—O(3)	2·03 (3)	Li(2a)—O(3)	1·80 (2)
Li(3)—O(1)	2·18 (2)	Li(4)—O(1)	2·108
Li(3)—O(1‴)	2·18 (2)	Li(4)—O(1′)	2·108
Li(3)—O(3)	2·14 (2)	Li(4)—O(3)	2·062
Li(3)—O(1″)	2·48 (2)	Li(4)—O(3′)	2·062
Li(3)—O(1′)	2·51 (2)	Li(4)—O(2)	2·497
Li(3)—O(2)	2·81 (2)	Li(4)—O(2′)	2·497

$Li_3Zn_{0.5}GeO_4$. Anisotropic B factors were refined for Ge and O, whereas the Li and Zn ions were constrained to isotropic thermal vibrations.

The final refinement terminated with $R_{wp} = 6{\cdot}73$ and $R_{ex} = 6{\cdot}84\%$ [for a definition of the R factors, see Rietveld (1969)]. The final refined atomic parameters for $Li_3Zn_{0.5}GeO_4$ are given in Table 1 with the derived bond lengths in Table 2; the fitted profile is shown in Fig. 1.*

Discussion

Structure of $Li_3Zn_{0.5}GeO_4$

The structure of $Li_3Zn_{0.5}GeO_4$ is most easily visualized by first considering the parent γ-Li_2ZnGeO_4 structure and then describing the formation of the interstitial solid solution from it. Considering first the structure of γ-Li_2ZnGeO_4, the basic framework consists of an oxide-ion array that is intermediate between hexagonal and tetragonal packing (West & Bruce, 1982). Within the oxide array the tetrahedral sites available for cations are arranged in face-sharing pairs but the centres of each pair are too close for simultaneous occupation of sites. The GeO_4 tetrahedra are isolated from each other, sharing only vertices with the $(Li/Zn)O_4$ tetrahedra. The tetrahedrally coordinated Li and Zn ions are, however, arranged in groups of three edge-sharing sites.

Formation of $Li_3Zn_{0.5}GeO_4$ involves replacement of a Zn^{2+} ion by two Li^+ ions, one of which occupies one of two octahedral interstitial sites, Li(3) or Li(4), while the other substitutes for the Zn^{2+} ion in a tetrahedral site. The tetrahedral site Li(2a), which is presumed vacant in Li_2ZnGeO_4, is partially occupied by lithium ions and is associated with vacancies on adjacent Li/Zn(2) sites. Li(3) and Li(4) sites share faces with fully or partially occupied tetrahedral sites; based on the random distribution of cations in the partially occupied sites, unfavourable cation repulsions would occur.

Although the neutron diffraction technique can yield only an average structure, close examination of the data coupled with a need to minimize cation repulsions, strongly supports a model involving short-range order, and in which two types of defect cluster, I and II, may be identified. The existence of defect clusters is to be anticipated in such a massively non-stoichiometric solid solution; indeed it has been proposed to account for the observed variation of conductivity with composition in lisicon solid solutions (Bruce & West, 1984). The overall structure of $Li_3Zn_{0.5}GeO_4$ consists of three substructures, one of which is identical to the structure of stoichiometric Li_2ZnGeO_4, the other two substructures are rich in lithium and consist of the two defect clusters I and II; the three substructures are shown in Figs. 2, 3 and 4.

(*a*) *Type*-I *cluster*. The cluster is comprised of one Li^+ in an octahedral Li(3) site, two tetrahedral sites [Li/Zn(2) and Li(2a)], which are each occupied by Li^+, and a vacant Li/Zn(2) site.

The Li(3) site shares two faces with Li/Zn(2) sites (Fig 3). In stoichiometric Li_2ZnGeO_4, all the Li/Zn(2) sites are presumed occupied, by analogy with the structure of γ-Li_3PO_4 (Zeman, 1960). In the interstitial solid solution the presence of a lithium ion on site (3) appears to promote displacement of a lithium ion from site (2) through the shared face into a (2a) tetrahedral site, thus reducing the unfavourable lithium repulsions associated with face-sharing

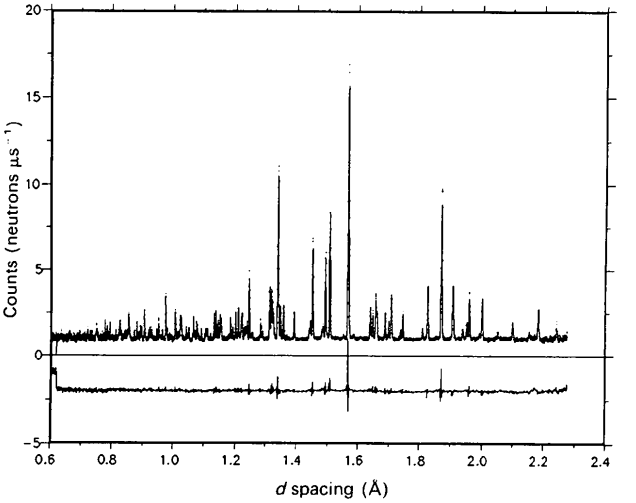

Fig. 1. Fitted powder neutron diffraction profile for $Li_3Zn_{0.5}GeO_4$, showing difference (obs. − calc.) plot. Key: obs. = points, calc. = solid lines.

* A list of numerical values corresponding to Fig. 1 has been deposited with the British Library Document Supply Centre as Supplementary Publication No. SUP 52143 (94 pp.). Copies may be obtained through The Executive Secretary, International Union of Crystallography, 5 Abbey Square, Chester CH1 2HU, England.

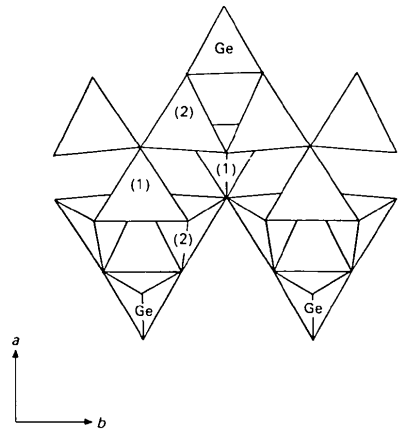

Fig. 2. c-Axis projection of the Li_2ZnGeO_4 substructure of $Li_3Zn_{0.5}GeO_4$. Unnamed tetrahedral sites contain Li and Zn ions. Li/Zn(1) and Li/Zn(2) sites are identified as (1) and (2), respectively.

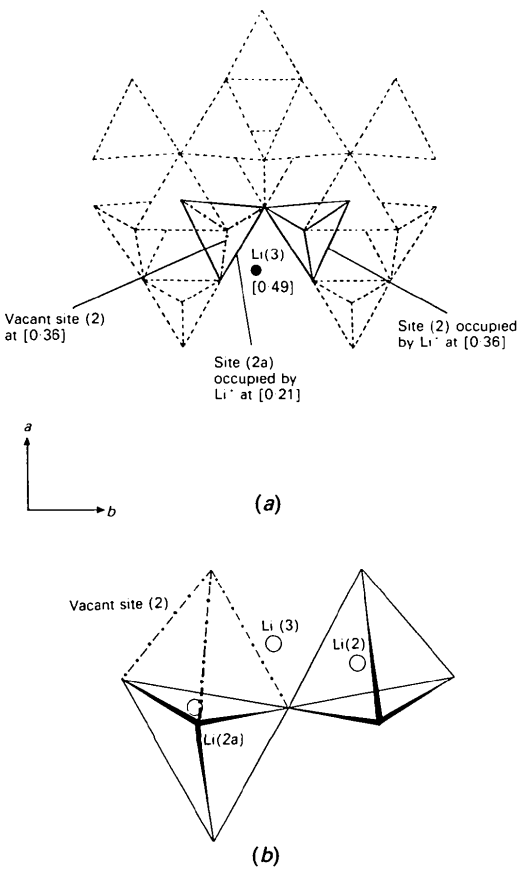

Fig. 3. (*a*) Projection as in Fig. 2 but with type-I defect cluster included. Tetrahedral sites delimited by dashed lines (---) indicate positions of surrounding sites not directly involved in the cluster. c-Axis heights are given in square brackets. Li/Zn(2) and Li(2a) sites are designated as (2) and (2a) respectively. (*b*) Alternative view of the type-I cluster indicating the relative position of the Li^+ cations.

sites. It is also anticipated that the other neighbouring Li/Zn(2) site is occupied by Li^+ rather than by Zn^{2+}, again based on repulsion considerations. Although Li(3) shares faces with two Li/Zn(2) sites, Li^+ ions are displaced from only one of these sites into a neighbouring (2a) site, as indicated by the similar occupancy of Li(3) and Li(2a) sites and the fact that Li(3) cations are not found at the centre of the octahedral site but in an eightfold position which is located off centre, closer to the face shared with the now empty Li/Zn(2) site (Fig. 3 and Table 1). The lithium ions occupying site 2(a) are located very close to the face shared with the Li/Zn(2) site and a movement of less than two e.s.d.'s is required to locate the ion in a five-coordinate site formed by combining the (2) and (2a) sites; however, we will regard the Li^+ ion as being located just within the (2a) site.

(*b*) *Type*-II *cluster*. This cluster consists of: three octahedral sites which are occupied by Li^+, two Li(3) and one Li(4); six tetrahedral sites also occupied by Li^+ cations, two Li/Zn(1), two Li/Zn(2) and two Li(2a); and finally, two vacant Li/Zn(2) sites.

The Li(4) site shares faces with two Li/Zn(2) sites, but in addition shares faces with two Li/Zn(1) sites (Fig. 4). It seems unlikely that an Li^+ ion would be located in an Li(4) site if all of these four neighbouring tetrahedral sites were occupied. There is no evidence for vacancies on the Li/Zn(1) sites but vacancies do exist on the Li/Zn(2) sites; thus it is anticipated that vacancies must occur on the Li/Zn(2) sites which share a common face with the Li(4)

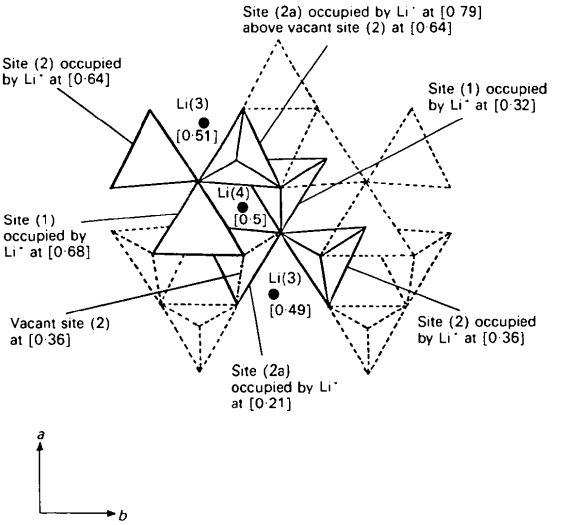

Fig. 4. Projection as in Fig. 2 including the type-II defect cluster. Tetrahedra delimited by dashed lines (---) indicate the positions of surrounding sites not directly involved in the cluster. c-Axis heights are given in square brackets. Li/Zn(1), Li/Zn(2) and Li(2a) sites are designated on the diagram by (1), (2) and (2a), respectively.

Table 3. *Refined cell and atomic parameters for* $Li_3Zn_{0.5}GeO_4$ *from constant-wavelength data with estimated standard deviations in parentheses*

	Position	x	y	z	B (Å^2)	Occupancy
Ge	4(*c*)	0·4138 (6)	0·25	0·3303 (9)	0·97 (9)	1
O(1)	8(*d*)	0·3363 (6)	0·0227 (7)	0·215 (1)	1·3 (1)	1
O(2)	4(*c*)	0·0876 (8)	0·75	0·170 (1)	1·0 (1)	1
O(3)	4(*c*)	0·0646 (7)	0·25	0·285 (1)	1·0 (1)	1
Li(1)	4(*c*)	0·429 (4)	0·75	0·168 (7)	2·1 (8)	0·89 (3)
Zn(1)	4(*c*)	0·429 (4)	0·75	0·168 (7)	2·1 (8)	0·11 (3)
Li(2)	8(*d*)	0·134 (10)	−0·007 (19)	0·325 (29)	2·1 (8)	0·63 (1)
Zn(2)	8(*d*)	0·134 (10)	−0·007 (19)	0·325 (29)	2·1 (8)	0·20 (1)
Li(2a)	8(*d*)	0·151 (8)	0·006 (13)	0·153 (19)	2·1 (8)	0·17 (2)
Li(3)	4(*c*)	0·202 (6)	0·25	0·037 (14)	2·1 (8)	0·27 (5)

sites. Examination of the occupancies of the Li(3) and Li(2a) sites [the latter of which accommodates Li^+ ions displaced from the Li/Zn(2) sites] suggests that on average one Li^+ ion is displaced by each Li(3) cation and that the octahedral Li(4) cations do not displace additional Li^+ ions from the Li/Zn(2) sites. However, once the Li/Zn(2) sites have been vacated, the adjacent Li(4) sites are suitable for occupation by Li^+. This points to a defect cluster which involves an Li(4) site sharing faces with two vacant Li/Zn(2) sites that in turn share faces with each of two Li(3) sites (Fig. 4).

Both the above defect structures avoid Li—Li contact distances of less than 1·98 Å and should therefore be quite stable, much more so than a random distribution of Li^+ cations which would require some closer Li—Li contacts. The driving force for formation of the clusters derives in part from the need to minimize cation repulsions and from the effective charge of −1 which arises as a result of the replacement of a framework Zn^{2+} ion by an Li^+ ion; this effective charge traps the octahedral Li^+ cations in the type-I and -II clusters.

The structural evidence suggests the existence of two defect clusters at the $Li_3Zn_{0.5}GeO_4$ composition; we believe that at low concentrations of interstitial ions (*i.e.* near the Li_2ZnGeO_4 composition) the simpler type-I cluster exists almost exclusively, but that with increasing non-stoichiometry and thus increasing lithium-ion concentration, the type-I clusters coalesce to form those of type II; this is consistent with the general observations in other non-stoichiometric compounds. The proposed model of defect clusters results in regions of the crystal devoid of zinc, with the composition 'Li_4GeO_4' and a structure involving octahedral and tetrahedral lithium ions, whereas other regions retain the structure and composition of the parent compound γ-Li_2ZnGeO_4. With increasing x the lithium-rich regions become more dominant until at $x = 1$ they would exist throughout the entire solid. It is worth noting that defect clusters have been proposed in a compound, $Li_{3.4}Si_{0.7}S_{0.3}O_4$ (Fitch, Fedner & Talbot, 1984), that is structurally similar to lisicon.

Comparison of the structures refined for lisicon using HRPD and D1A

It is instructive to compare the structure refinement of $Li_3Zn_{0.5}GeO_4$ using our recent HRPD data with that previously obtained from the D1A diffractometer. Table 3 shows the refined data using the constant-wavelength technique. The basic framework of Ge and O atoms is very similar in both neutron refinements; however, there are significant differences in the lithium distribution. Using D1A:

(*a*) Lithium could not be located on the Li(4) site.

(*b*) Li(3) was located in a fourfold position with lower occupancy.

(*c*) The lithium positions in sites (2) and (2a) were not well determined.

In the previous refinement the presence of a small amount of Li on the Li(4) site was only observed in the case of the $x = 0{\cdot}75$ material. The amount of Li in site (4) in the present study, although large compared with the e.s.d.'s obtained using HRPD, is comparable with the e.s.d.'s obtained for lithium ions in our D1A data, thus precluding the identification of the Li(4) site. It is noteworthy that the Li(4) B factor and occupancy exhibit a correlation of approximately 35% when refined using HRPD; this compares well with a number of correlations between positional parameters of other atoms.

In the D1A study the Li(3) site was fixed at the 4(*c*) special position; attempts to refine the y coordinate resulted in a value close to 0·25.

The positional parameters of Li(2) and especially Li(2a) are significantly shifted away from those reported earlier. This is not unexpected as the e.s.d.'s on these positions in the earlier work were very much higher than on any of the other atoms.

Anisotropic thermal parameters could not be refined to give meaningful values from the D1A data, whereas using HRPD this was achieved for Ge and O. The thermal parameters for the lithium and zinc ions, which were extensively tied together during the refinement of the D1A data, have been largely decoupled with HRPD.

In general, as indicated by examining the e.s.d.'s in Tables 1 and 3, the atomic parameters are better determined in the case of HRPD. This is largely due to the higher resolution of this instrument compared to D1A and the far greater number of reflections (860 for HRPD, 214 for D1A) obtained with the much lower d-spacing limit (0·4 Å for HRPD, 1·0 Å at $\lambda = 1{\cdot}909$ Å for D1A). It is evident that the HRPD data clearly approach those available in a single-crystal X-ray structure determination. In particular, it may be seen that for compounds in which the cations are distributed over a number of crystallographically distinct sites, as is the case for the lisicon solid solutions, HRPD offers a significantly better refinement indicating important structural

differences which although subtle are critical to an understanding of ionic conduction.

The above discussion is not intended to imply that constant-wavelength instruments are in general inferior to those based on time-of-flight. 'State-of-the-art' constant-wavelength instruments such as D2B would, we are sure, offer a considerably improved refinement to that from D1A, probably comparable in many respects to HRPD.

Finally, it is noteworthy that the X-ray structure determination (Plattner & Völlenkle, 1979) failed to identify the displaced Li(2a) cations or the existence of the second lithium site (4); this may be attributed to the weak scattering of X-rays by lithium ions.

We wish to thank R. M. Ibberson at the Neutron Division, Rutherford–Appleton Laboratory, England, for his help with data collection; the Computer Centre at Heriot-Watt University for provision of computer facilities for carrying out the refinements; and the SERC for financial support.

References

ABRAHAMS, I., BRUCE, P. G., DAVID, W. I. F. & WEST, A. R. (1988). *J. Solid State Chem.* **75**(2), 390–396.
BRUCE, P. G. & WEST, A. R. (1980). *Mater. Res. Bull.* **15**, 379–385.
BRUCE, P. G. & WEST, A. R. (1982). *J. Solid State Chem.* **44**, 354–365.
BRUCE, P. G. & WEST, A. R. (1984). *J. Solid State Chem.* **53**, 430–434.
DAVID, W. I. F., AKPORIAYE, D. E., IBBERSON, R. M. & WILSON, C. C. (1988). *The High Resolution Powder Diffractometer at ISIS – an Introductory Users Guide*, version 1.0. Rutherford–Appleton Laboratory, England.
FITCH, A. N., FENDER, B. E. F. & TALBOT, J. (1984). *J. Solid State Chem.* **55**, 14–22.
HONG, Y.-P. (1978). *Mater. Res. Bull.* **13**, 117–124.
International Tables for Crystallography (1983). Vol. A. Dordrecht: Kluwer Academic Publishers.
KOESTER, L. & RAUCH, H. (1981). Report 2517/RB. International Atomic Energy Agency, Vienna.
PLATTNER, E. & VÖLLENKLE, H. (1979). *Monatsh. Chem.* **110**, 693–698.
RIETVELD, H. M. (1969). *J. Appl. Cryst.* **2**, 65–71.
RODGER, A. R., KUWANO, J. & WEST, A. R. (1985). *Solid State Ionics*, **15**, 185–198.
WEST, A. R. & BRUCE, P. G. (1982). *Acta Cryst.* B**38**, 1891–1896.
ZEMAN, J. (1960). *Acta Cryst.* **13**, 863–867.

Acta Cryst. (1989). B**45**, 462–466

Structural Analysis of the Threefold-Modulated Monoclinic Phase of $[N(CH_3)_4]_2ZnCl_4$

BY F. J. ZÚÑIGA, G. MADARIAGA AND J. M. PÉREZ-MATO

Departamento de Fisica de la Materia Condensada, Facultad de Ciencias, Universidad del Pais Vasco, Apdo 644 *Bilbao, Spain*

(*Received* 9 *September* 1988; *accepted* 8 *May* 1989)

Abstract

The crystal structure of the threefold monoclinic low-temperature phase of bis(tetramethylammonium) tetrachlorozincate(II), $[N(CH_3)_4]_2ZnCl_4$, has been studied at 250 and 200 K. The R values are 0·062 (6893 reflections, 3616 observed) and 0·064 (1907 reflections, 1558 observed) at 250 and 200 K respectively. The distortion with respect to the high-temperature phase is analyzed in terms of symmetry modes, and compared with the distortion in the incommensurate phase. The mode with Σ_3 symmetry responsible for the normal–incommensurate transition is still predominant in the distortion. Crystal data: $M_r = 355{\cdot}5$, λ(Mo $K\alpha$) = 0·7107 Å, $P2_1/n$, $Z = 12$, $F(000) = 2208$. At 250 K: $a = 8{\cdot}953\ (3)$, $b = 15{\cdot}456\ (10)$, $c = 36{\cdot}595\ (8)$ Å, $\gamma = 90{\cdot}19\ (4)^\circ$, $V = 5064\ (6)$ Å^3, $D_x = 1{\cdot}40$ g cm^{-3}, $\mu = 20{\cdot}7$ cm^{-1}. At 200 K: $a = 8{\cdot}960\ (2)$, $b = 15{\cdot}309\ (5)$, $c = 36{\cdot}628\ (8)$ Å, $\gamma = 90{\cdot}46\ (2)^\circ$, $V = 5024(4)$ Å^3, $D_x = 1{\cdot}41$ g cm^{-3}, $\mu = 21{\cdot}0$ cm^{-1}.

0108-7681/89/050462-05$03.00

1. Introduction

Bis(tetramethylammonium) tetrachlorozincate (TMATC-Zn) is one of the most studied compounds of the A_2BX_4 family having a one-dimensional incommensurate (INC) phase. This compound undergoes five solid–solid phase transitions:

$$\text{I} \xrightarrow[T_i]{297\ \text{K}} \text{II} \xrightarrow[T_c]{281\ \text{K}} \text{III} \xrightarrow{277\ \text{K}} \text{IV} \xrightarrow{171\ \text{K}} \text{V} \xrightarrow{159\ \text{K}} \text{VI},$$

where the temperatures are those obtained from calorimetric measurements by Ruiz-Larrea, Lopez-Echarri & Tello (1981).

Diffraction patterns of phases II, III and IV show superstructure reflections along the **c*** direction that correspond to periodicities of $\sim 5c_0$ (INC), $5c_0$ and $3c_0$ respectively, c_0 being the lattice constant of phase I (Tanisaki & Mashiyama, 1980). These satellite reflections are all weak and the structures can be considered small distortions of the parent phase I.